© 2017. Published by The Company of Biologists Ltd | Journal of Experimental Biology (2017) 220, 4399-4409 doi:10.1242/jeb.163436

RESEARCH ARTICLE

Plastic responses of bryozoans to ocean acidification

Daniel S. Swezey[1,*], Jessica R. Bean[2,3], Tessa M. Hill[1,2], Brian Gaylord[1,4], Aaron T. Ninokawa[1] and Eric Sanford[1,4]

ABSTRACT

Phenotypic plasticity has the potential to allow organisms to respond rapidly to global environmental change, but the range and effectiveness of these responses are poorly understood across taxa and growth strategies. Colonial organisms might be particularly resilient to environmental stressors, as organizational modularity and successive asexual generations can allow for distinctively flexible responses in the aggregate form. We performed laboratory experiments to examine the effects of increasing dissolved carbon dioxide (CO_2) (i.e. ocean acidification) on the colonial bryozoan *Celleporella cornuta* sampled from two source populations within a coastal upwelling region of the northern California coast. Bryozoan colonies were remarkably plastic under these CO_2 treatments. Colonies raised under high CO_2 grew more quickly, investing less in reproduction and producing lighter skeletons when compared with genetically identical clones raised under current surface atmosphere CO_2 values. Bryozoans held under high CO_2 conditions also changed the Mg/Ca ratio of skeletal calcite and increased the expression of organic coverings in new growth, which may serve as protection against acidified water. We also observed strong differences between source populations in reproductive investment and organic covering reaction norms, consistent with adaptive responses to persistent spatial variation in local oceanographic conditions. Our results demonstrate that phenotypic plasticity and energetic trade-offs can mediate biological responses to global environmental change, and highlight the broad range of strategies available to colonial organisms.

KEY WORDS: Phenotypic plasticity, Acclimatization, Colonial growth forms, Calcification, Global environmental change, Regional oceanography

INTRODUCTION

Evaluating the capacity of plant and animal species to acclimatize and/or adapt to global environmental change is central to efforts to predict the biological consequences of anthropogenic disturbances (Jump and Penuelas, 2005; Hoffmann and Sgrò, 2011; Munday et al., 2013). Phenotypic plasticity may play a crucial role in buffering organisms against the deleterious effects of global environmental change, potentially allowing time for genetic adaptation (Chevin et al., 2010; Munday et al., 2013). Although infrequently explored, the role of phenotypic plasticity may be especially pronounced in clonal and colonial organisms. Colonial organisms produce successive sets of modular units through time, allowing for adaptive shifts in phenotypes across asexual generations (Hughes, 2005). Units in colonies are also interconnected, allowing for diverse strategies of resource distribution (Alpert, 1991) and adaptive changes in allocation to different areas of the colony in response to environmental stress (Callaghan et al., 1992; Stuefer, 1996). Finally, colonial taxa employ both asexual and sexual modes of reproduction, often exhibiting distinctive flexibility in the timing and modes of reproduction, allowing for the delay or acceleration of sexual reproduction as a risk-spreading strategy to maximize fitness when challenging environmental conditions prevail (Harvell and Grosberg, 1988; Callaghan et al., 1992).

The response of an individual clonal unit to environmental change can be dictated by a variety of biological factors, including its position in the colony and age (Hutchings and Bradbury, 1986; McKinney and Jackson, 1989), the level of physiological integration of the units in the colony (Hutchings and Wijesinghe, 1997), and possibly developmental canalization, i.e. the tendency for a given genotype to produce a fixed phenotype, regardless of variability in the environment (Waddington, 1942). These biological factors, along with the strength and duration of environmental signals, determine the responses of particular units within a colony (McKinney and Jackson, 1989; Callaghan et al., 1992; Sánchez et al., 2007). Colonial organisms can be thought of as variations on a single theme, with modularity and phenotypic plasticity allowing clones in a colony to couple or decouple from the developmental history of prior asexual generations, resulting in a flexible aggregate form that may make the colony as a whole more resilient to environmental stress.

In this study, we explored whether phenotypic plasticity mediates the responses of bryozoan colonies to ocean acidification. Bryozoans are collections of genetically identical units (termed zooids) that are formed sequentially through time via asexual budding. Because most bryozoans are sessile, with encrusting species expanding laterally during growth, physiological plasticity in response to environmental change can be observed within colonies across the continuous time sequence of zooid growth and development. Bryozoan colonies can also be subdivided to create assemblages of genetically identical replicate clones, which can then be assigned to separate treatments (Hughes and Hughes, 1986), allowing for statistical designs where variation associated with particular familial lineages and replicate genotypes can be included as model variance components.

Ocean acidification and the California Current

Calcifying marine organisms are increasingly threatened by ocean acidification (OA). The world's oceans have absorbed at least one-third of the anthropogenic carbon dioxide (CO_2) emissions released to the atmosphere since the beginning of the Industrial Revolution (Sabine et al., 2004). The absorption of this CO_2 has reduced average surface water pH in the global ocean by at least 0.1 pH units

[1]Bodega Marine Laboratory, University of California, Davis, 2099 Westshore Road, Bodega Bay, CA 94923, USA. [2]Department of Earth and Planetary Sciences, University of California, Davis, One Shields Ave, Davis, CA 95616, USA. [3]University of California Museum of Paleontology, University of California, Berkeley, CA 94720-4780, USA. [4]Department of Evolution and Ecology, University of California, Davis, One Shields Ave, Davis, CA 95616, USA.

*Author for correspondence (dsswezey@ucdavis.edu)

D.S.S., 0000-0003-2560-249X

Received 23 May 2017; Accepted 18 September 2017

Journal of Experimental Biology (2017) 220, 4399-4409 doi:10.1242/jeb.163436

compared with pre-industrial values, and reductions are projected to accelerate in coming years, with a decline of 0.3–0.5 pH units by 2100 (Caldeira and Wickett, 2005).

Along portions of the west coast of North America, patterns of wind stress and nearshore ocean circulation result in the coastal upwelling of deep oceanic low-pH waters during spring and summer months (Feely et al., 2008). Sensor data collected over the last decade indicate that coastal habitats in northern California experience periods of low-pH conditions during upwelling, with pH values frequently dropping below 7.8, accompanied by low $CaCO_3$ saturation states (Feely et al., 2008; Hofmann et al., 2014; Chan et al., 2017). Paleoceanographic data suggest that similar upwelling conditions have been a persistent feature of the northern California Current Large Marine Ecosystem (CCLME) for thousands of years (Jacobs et al., 2004). Moreover, models suggest that acidification of the CCLME is expected to be one of most rapid and substantial modern chemical changes in the world's surface ocean, with chronic low-pH conditions projected by 2050 (Gruber et al., 2012).

As oceans become more acidic, the concentration of carbonate ions in seawater decreases, potentially making the formation of shells and skeletons more difficult for calcifying species (Orr et al., 2005). Acidification can also alter the energetics of proton exchange between intra- and extra-cellular compartments, incurring energetic costs and disrupting basic cellular processes (Pörtner, 2008). Recent results, primarily from short-term laboratory exposures, suggest that OA negatively impacts growth and calcification in a variety of marine taxa (Kroeker et al., 2013). However, despite the potential for a wide array of ecological consequences (Gaylord et al., 2015), few studies have quantified whether plastic responses in colonial animals might reduce their susceptibility to these near-future conditions.

Study system: California bryozoans

We studied plastic responses to OA exhibited by *Celleporella cornuta* (Busk 1854), a calcified encrusting colonial bryozoan native to intertidal and subtidal habitats of coastal California (Morris, 1980). *Celleporella cornuta* colonies are derived from sexually produced swimming larvae, which settle on benthic surfaces (typically macroalgae) and asexually bud to produce colonies composed of inter-connected units (zooids). Mature colonies possess both male and female reproductive zooids, and non-sexual feeding zooids.

We conducted a long-term laboratory experiment to test the hypothesis that although bryozoans may be sensitive to near-future OA, they also possess a plastic capacity to manipulate colony form and function to minimize the impacts of OA. We used lineages of *C. cornuta* clones sampled from two northern Californian populations to test three specific predictions: (1) colonies raised under high CO_2 conditions (low pH, low $CaCO_3$ saturation state) will show reduced growth and calcification as a result of the negative degradation effects of OA; (2) colonies raised under high CO_2 conditions will display stress-related energetic trade-offs by varying the proportion of zooids allocated to feeding versus reproduction as a plastic compensatory response to OA; and (3) individuals within and among colonies will reduce investment in calcification and alter the mineralogical composition of skeletal calcite under high CO_2 conditions as a plastic compensatory response to OA.

MATERIALS AND METHODS

Oceanographic sampling

To characterize regional trends in pH conditions experienced by colonies in the field, we placed autonomous sensors containing Durafet® pH electrodes (Martz et al., 2010) in the low intertidal habitat where bryozoans were collected at our two study sites: Van Damme State Park (VD; 39°17′3.24″N, 123°48'5.05″W) near Mendocino, CA, USA, and the Bodega Marine Reserve (BMR; 38° 19′6.72″N, 123°4′26.88″W) in Bodega Bay, CA, USA. From 2010 to 2013, we collected simultaneous pH (total scale) and temperature data (at 10-min intervals) at these locations during April through September, which is when *C. cornuta* reproduces and recruits along the California coast (Morris, 1976). From these sensor data, we also calculated aragonite saturation state values ($\Omega_{aragonite}$), a measure of the thermodynamic potential for $CaCO_3$ to precipitate or dissolve in solution, which is dependent on both the temperature of seawater and dissolved Ca^{2+} and CO_3^{2-} concentrations. We also calculated the incidence of low $CaCO_3$ saturation state conditions falling below $\Omega_{aragonite}<1.7$, a threshold observed to be detrimental in other temperate taxa (Barton et al., 2012; Chan et al., 2017). See Appendix for further detail on sensor deployments and saturation state calculations.

To quantify potential differences in phytoplankton concentrations associated with oceanographic variation at these sites, we determined surface chlorophyll *a* (chl *a*) concentrations at both sites using a 16-year dataset of satellite imagery (spanning 1999–2015). In 2013, we also collected bottle samples from shore to assess chl *a* concentrations at these sites. See Appendix for further detail on methodologies.

Collections, spawning and laboratory culture

Fifty *C. cornuta* colonies with gravid reproductive zooids (ovicells) were collected on low-intertidal red algal blades (*Mazzaella* spp. and *Rhodymenia* sp.) from BMR and VD during fall 2012. Colonies were transported to the Bodega Marine Laboratory and spawned to generate F1 offspring for experiments (see Appendix for spawning and culture techniques). All experiments were approved by the administration of the UC Davis Bodega Marine Laboratory. These offspring were then propagated for 6 months under common garden conditions (400 µatm CO_2, 15.3°C), generating 68 reproductively mature colonies. Two genetic clones of each genotype were then generated by dividing colonies evenly in two, resulting in a total of 134 experimental colonies representing 68 genotypes and 20 maternal families across the two populations.

Each clone from a genetic replicate pair was then randomly assigned to either a high-CO_2 or low-CO_2 treatment, such that each replicated genotype was simultaneously exposed to both experimental conditions. Treatments were maintained using a custom-designed flow-through OA system (see Appendix for system details). Colonies were photographed under a stereo microscope (Leica M125 with a Leica DC290 camera; Leica Microsystems, Wetzlar, Germany) to quantify the number and condition of the zooids comprising each colony at the end of the common garden phase. Individuals assigned to the high-CO_2 treatment were then gradually exposed to reduced pH conditions by adding 200 µatm of CO_2 every other day to the air mixture being delivered to the high-CO_2 sump. This CO_2 ramp was performed for 8 days until the air mixture contained approximately 1150 µatm of CO_2, generating an experimental *in situ* $\Omega_{aragonite}$ of 0.98, matching partial pressure of CO_2 (P_{CO_2}) and saturation state values experienced by field colonies during peak upwelling events (Chan et al., 2017). After 8 weeks under the experimental conditions, the colonies were photographed again, and colony growth was quantified by comparing the initial and final images. See Appendix for additional details on experimental culture protocol.

Journal of Experimental Biology

Journal of Experimental Biology (2017) 220, 4399-4409 doi:10.1242/jeb.163436

Analysis of colony composition and skeletal mass

To quantify changes in colony growth and reproductive investment over the course of the 8-week experimental period (hereafter referred to as the treatment phase), we used image analysis software (ImageJ v1.48) to quantify zooid forms in *C. cornuta* colonies at the beginning and the end of this period, following Pistevos et al. (2011). Each zooid in each colony was classified into one of five categories: (1) active feeding autozooids (A_F), (2) degenerated autozooids (known as 'brown bodies') (A_B), (3) male zooids (A_M), (4) female zooids (ovicells) (O) and (5) incomplete zooids that were still forming when the image was taken. Based on morphological descriptions (Morris, 1980) and our observations, we determined that *C. cornuta* autozooids exist in one of three states: autozooids, with a well-developed lophophore with many tentacles and usually a gut containing phytoplankton; a non-feeding male state, with a reduced lophophore and developing sperm; and a degenerated zooid state known as a brown body, indicated by the degeneration of the lophophore and gut, leaving a darkened remnant. In bryozoans, stressful conditions are known to trigger the degeneration of active zooids to the brown body state as a means of energy conservation (Gordon, 1977). Autozooids in this species thus appear to exist in an interchangeable balance among these three phases, and, during this study, some individual zooids were observed to transition from feeding autozooids to males, and then back again.

At the beginning and conclusion of the treatment phase, we also observed and quantified the production of organic coverings on colony autozooids (A_C) and ovicells (O_C) (Fig. 1). Although previously observed in this species (Morris, 1980), this morphological response is poorly understood. Evidence suggests that these zooid coverings consist of both organic and calcified components, and may be extensions of the organic cuticle (Morris, 1980; Taylor et al., 2015). At the conclusion of the experiment, we also weighed whole colonies and regressed both organic and ash-free carbonate mass against the final number of colony autozooids to estimate the average organic and carbonate mass per autozooid (see Appendix for additional methods).

Statistical analyses

Using data compiled from our photo record, we modeled five growth response variables using a linear mixed effects model implemented in JMP PRO v12. (1) The total number of new zooids of all five types added during the treatment phase. (2) $A_B/(A_F+A_M+A_B)$: the number of zooids in a degenerated (brown body) state in a given colony over the total number of living autozooids of all forms. An increase in this ratio indicates a decrease in overall colony condition. (3) $\log_{10}(O+1)/[(A_F+A_M+A_B)+1]$: female reproductive investment, or the log ratio of the number of ovicells added during the treatment phase over the number of autozooids added. Values of this index will increase with increasing numbers of ovicells relative to autozooids and decrease with increasing numbers of autozooids relative to ovicells, and is zero for equal numbers of either type. This index is analogous to a gonado-somatic index, applied to growth added during the treatment phase. (4) $A_M/(A_M+A_F)$: the number of males distributed throughout the entire colony at the end of the treatment phase over the total number of males and feeding autozooids. An increase in this ratio indicates an increase in male reproductive investment. (5) $(A_C+O_C)/(A_F+A_M+A_B+O)$: the ratio of zooids that grew new organic coverings during the treatment phase. The occurrence of new organic covering formation was quantified in both new growth (zooids added during the treatment phase) and old growth (original colony zooids that grew before treatment phase).

To reduce the effects of outliers, response variables were winsorized at the 5% and 95% level for each of the four population×CO_2 groupings using the residual distributions of each model. We performed *t*-tests based on residual maximum likelihood conditional estimates of the variances to determine the significance of each fixed effect coefficient against the other fixed effects in the models (Pinheiro and Bates, 2000), followed by subsequent *t*-tests on pairwise comparisons of the least squares means estimates for different levels within our main effect structure (for full model output, see Table S2). Where applicable, we tested model assumptions by plotting the residuals versus the fitted values, and used Levene's test for homogeneity of variance, and Shapiro–Wilk test for normality.

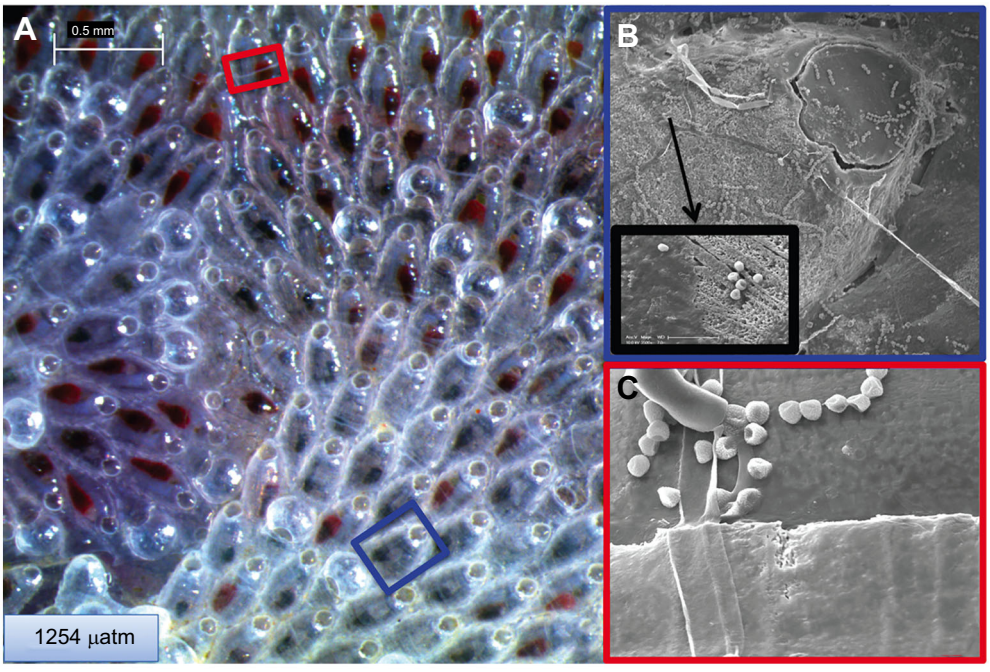

Fig. 1. Morphological changes through time in a *Celleporella cornuta* colony exposed to high CO_2. (A) Colored boxes over colony zooids highlight changes in zooids of interest, magnified in B and C under scanning electron microscopy (SEM). (B) Under high CO_2, the organic cuticle is reduced, and the calcite skeleton is exposed. Arrow in B points to box magnifying a region of a zooid surface where a receding cuticle is observed, revealing the inner calcified surfaces of exterior walls. This phenomenon was primarily observed in older zooid generations that formed prior to exposure to the high CO_2 treatment. (C) Later asexual generations showed signs of acclimation, forming new organic coverings that appear as an elevated plane in the lower half of the image. These layers grew and encapsulated outer zooid surfaces after exposure to high CO_2. The small spheres observed under SEM are likely cyanobacteria growing on the surface of the zooid.

Journal of Experimental Biology (2017) 220, 4399-4409 doi:10.1242/jeb.163436

For the first response variable (total zooids added), the initial number of resource-collecting feeding autozooids at the start of the treatment phase was used as a covariate in our model. This covariate was crossed with all fixed and random factors in the analysis to account for initial differences in colonies ability to acquire food, which might affect overall zooid production rates. Our models partitioned variation by maternal family and clone genotypes in each treatment, and we used this nesting structure for all applicable analyses. Our model included the following fixed/random effects (where R indicates model factors that were treated as random effects): population; family [population] (R); genotype [family [population] (R); CO_2 level; CO_2×population; CO_2×family [population] (R); and residual error (R).

Skeletal magnesium and thickness analysis

As the Mg content of biogenic calcite increases, skeletal calcification becomes increasingly soluble and thus more vulnerable to dissolution under low pH conditions (Morse et al., 2006; Swezey et al., 2017). To test for shifts in skeletal composition related to OA exposure, we analyzed molar magnesium to calcium ratios (Mg/Ca_C) from zooid calcite, taking measurements from eight sequentially grown zooids from a clonal replicate pair from the VD population (n=16 zooids total). One clone was exposed to low CO_2 whereas the replicate clone was exposed to the high-CO_2 treatment. At the conclusion of the experiment, each colony was embedded in epoxy and finely polished to expose sagittal sections of zooids for quantitative elemental spot analysis. All zooids analyzed from both colonies were grown under the same temperature (15.3°C) during the treatment phase. Elemental analyses were carried out using an electron microprobe (Cameca SX-100, Gennevilliers, France). Prior to each run, the instrument was calibrated on calcite and celestine standards. Software (Cameca PeakSight 4.0, Gennevilliers, France) determined standard-based corrections were then applied to the data, and drift offsets subtracted. Mg and Ca concentrations were quantified using 1 µm spots (15 kV, 20 nA beam) distributed evenly across the upper rim of the primary frontal wall of each zooid. Mol% element data were then generated from these sample points. Patterns in the distribution of Mg in the calcified walls of autozooids from these clones were further visualized using X-ray element maps (Fig. 2). We also measured the thickness of the calcified walls of zooids using scanning electron microscopy (SEM) images of the zooid sagittal sections, measuring the thickness of walls every 40 µm along the upper rims of zooids, collecting an average of 10 measurements per zooid.

Monitoring of seawater chemistry and temperature

Throughout the experiment, we measured the pH (total scale) of seawater in treatment sumps five times per week and sampled for total alkalinity (TA) on three days each week. Each week, we also recorded *in situ* conditions in a random sample of experimental containers bearing individual bryozoan colonies. During the course of the experiment, total alkalinity was sampled from our treatment sumps via automated Gran titration (Metrohm 809 Titrando), standardized using certified reference material from A. Dickson at Scripps Institute of Oceanography. Temperature-corrected seawater pH from our treatment sumps and experimental containers was quantified using a potentiometric pH/temperature meter (Accumet Excel XL60). Sump salinity was determined using a multi-parameter instrument (YSI 6600V2, YSI, Yellow Springs, OH, USA). During the treatment phase, pH was further quantified using a Sunburst Submersible Autonomous Moored Instrument (SAMI) spectrophotometric pH sensor that was adapted for laboratory benchtop use. This SAMI instrument recorded pH in total scale using spectrophotometric characterization of m-Cresol Purple. We calibrated the Accumet XL probe measurements in total scale (Easley and Byrne, 2012) using the total scale pH determined by the SAMI along with the temperature and salinity of the sumps and incoming seawater.

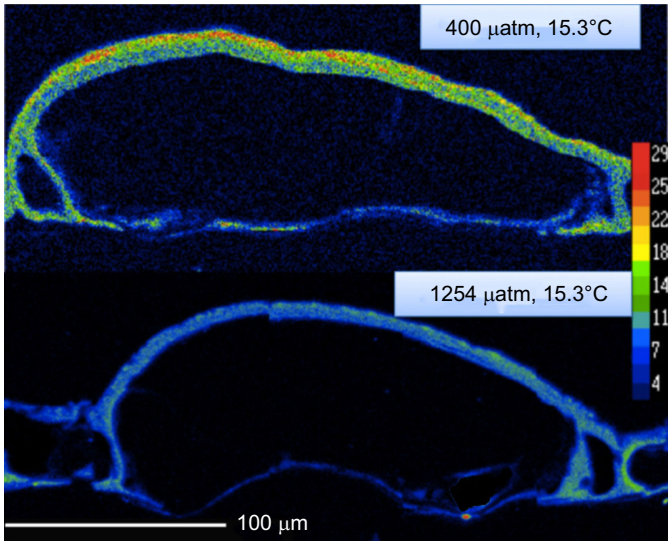

Fig. 2. Magnesium (Mg) content of skeletal walls in sagittal sections of *Celleporella cornuta* zooids from high and low CO_2 treatments. Mg concentration maps were generated using electron microprobe analyses of the skeletal walls of individual autozooids from genetic replicates. The Mg concentration scale to the right represents the range of X-ray counts collected by the electron microprobe from samples, including a small proportion of background counts. Warmer colors indicate higher Mg concentrations. Mg concentrations in the calcite of skeletal walls were higher in zooids grown under current atmospheric CO_2 values (top) than under high CO_2 (bottom). A thinning of zooid walls is also apparent under high CO_2.

To verify that conditions in our treatment sumps did not vary substantially from conditions in our experimental containers, we measured pH once per week in 14 randomly chosen experimental containers (seven from each treatment) using the calibrated Accumet XL instrument. We used these total scale pH data and sump alkalinity measurements to calculate $\Omega_{calcite}$ and $\Omega_{aragonite}$ values in containers during the 2-month experimental CO_2 treatment. Before the treatment phase, we also compared the alkalinity of the water in six to 10 randomly selected experimental containers (just prior to container changes) to alkalinity values in the source sump once per week for 8 weeks. No significant differences were found between and among sumps or containers during these trials, and so alkalinity variation amongst containers was assumed to be minimal during our experiment. Temperatures in three experimental containers per manifold were recorded every 15 min using data loggers (Hobo Tidbit v2, Onset Computer, Bourne, MA, USA). These containers received dripping seawater from the treatment sump(s), and were distributed evenly among the containers housing bryozoan colonies.

RESULTS

Laboratory and field variation in seawater pH, carbonate chemistry, and chlorophyll content

Mean laboratory pH (and P_{CO_2}) during the experiment were calculated to be 8.04 (400 µatm) and 7.60 (1254 µatm), with associated $\Omega_{aragonite}$ of 2.34 and 0.98 for the low and high CO_2 treatments, respectively (see Appendix, Table S1). The mean

Journal of Experimental Biology (2017) 220, 4399-4409 doi:10.1242/jeb.163436

temperature in experimental containers held on the seawater table was 15.3°C for both treatments.

VD and BMR field sites experienced 3-year average $\Omega_{aragonite}$ values of 1.73 and 1.92, respectively. Mean (±s.d.) pH at these sites were similar across years (VD=7.99±0.09; BMR=8.00±0.13), whereas mean (±s.d.) temperatures were approximately 1.5°C cooler at VD (VD=10.25±1.28°C; BMR=11.70±1.52°C). Low saturation states were more frequently observed at VD, with 54% of intertidal sensor measurements falling below $\Omega_{aragonite}$ of 1.7, as compared with 43% at BMR.

Surface chlorophyll level estimates from our 16-year record of satellite data differed between sites (t_{489}=−7.286, P<0.0001), with BMR exhibiting a mean concentration of 6.78 mg m^{-3} (95% CI=6.13, 7.43), roughly double the mean of 3.36 mg m^{-3} observed at VD (95% CI=2.71, 4.01). Measurements from bottle samples taken during the summer of 2013 were consistent with this trend, with average chl *a* concentrations being between 1.8 and 6.3 times greater at BMR than VD on each monthly sample date, with an average concentration of 13.82 mg m^{-3} (95% CI=10.81, 16.83) at BMR versus 3.77 mg m^{-3} (95% CI=0.76, 6.78) at VD.

Effects on colony growth and skeletal mass

Under high CO_2, clones from both VD and BMR populations exhibited faster growth (more zooids added during the experiment) than clones held under low CO_2 (Fig. 3). Total zooids added varied with the interaction terms CO_2×initial autozooids and population×initial autozooids (P=0.032 and P=0.019, respectively) with VD–high CO_2 adding more zooids compared with all other groups (BMR–low CO_2: P=0.005; BMR–high CO_2: P=0.016; VD–low CO_2: P=0.047).

Colony reproductive investment varied significantly with CO_2, with investment in both female and male reproductive zooids declining under high CO_2 (P=0.003 and P=0.044, respectively; Fig. 4). Female zooid investment was significantly reduced in VD–high CO_2 compared with VD–low CO_2 (P=0.034), and BMR–high CO_2 compared with BMR–low CO_2 (P=0.031). There was also suggestive evidence that the proportion of males in colonies was reduced in BMR–high CO_2 compared with BMR–low CO_2 (P=0.087), although this trend was not observed in the VD population (P=0.235). CO_2 also had a significant effect on the percentage of degenerated zooids observed in colonies (P=0.034). Both populations had a greater proportion of degenerated zooids under high CO_2, but significant differences between CO_2 levels were only observed in the BMR population (P=0.044).

Under low CO_2, bryozoan colonies were predominantly $CaCO_3$ with small amounts of organics which comprised approximately 15–17% of zooid mass (Fig. 5). Compared with clones in the low CO_2 treatment, high CO_2 zooids from BMR contained 31% less

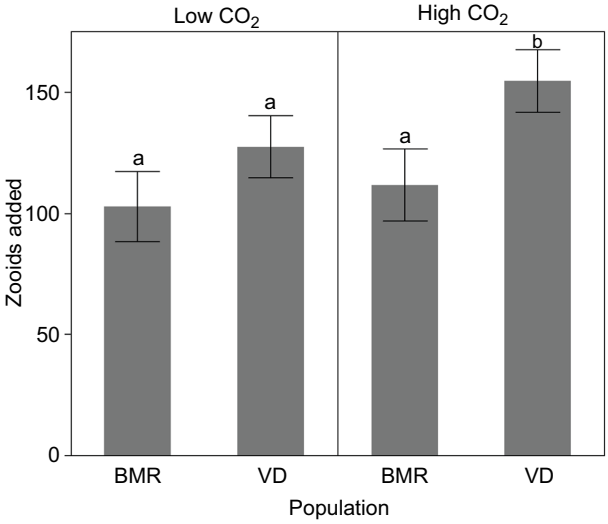

Fig. 3. Growth of *Celleporella cornuta* colonies under low and high CO_2 treatments. Figure shows least squares group means for total zooids added in colonies from both populations during the 2-month treatment phase. Shared letters indicate group means that are not significantly different based on means comparisons of least squares group estimates (P>0.05). Error bars are ±1 s.e.m. BMR, Bodega Marine Reserve; VD, Van Damme State Park. Sample sizes: VD–high CO_2 n=38, VD–low CO_2 n=39, BMR–high CO_2 n=28, BMR–low CO_2 n=29.

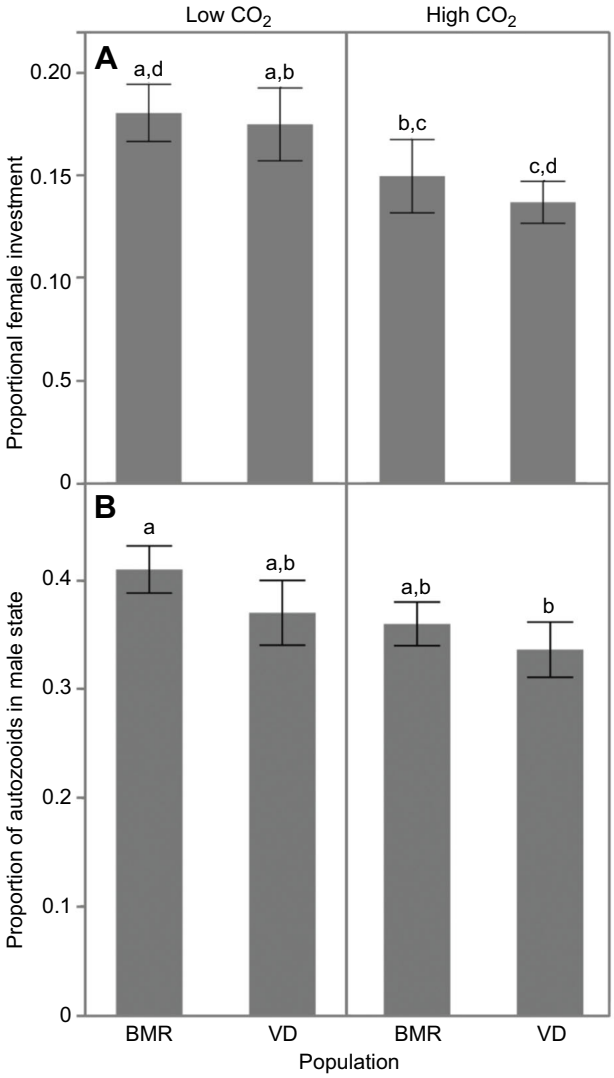

Fig. 4. Differences in reproductive investment in *Celleporella cornuta* under low and high CO_2. (A) The proportion of zooids added that were non-feeding female ovicells at the end of the treatment phase. (B) The proportion of non-feeding males amongst non-degenerated autozooids in the colonies. Under high CO_2, a reduction in ovicell investment (after accounting for the number of autozooids produced) and a declining proportion of males in colonies was observed in both populations. Shared letters indicate group means that are not significantly different based on means comparisons of least squares group estimates (P>0.05). Error bars are ±1 s.e.m. Sample sizes: VD–high CO_2 n=38, VD–low CO_2 n=39, BMR–high CO_2 n=28, BMR–low CO_2 n=29.

Journal of Experimental Biology (2017) 220, 4399-4409 doi:10.1242/jeb.163436

$CaCO_3$, and high CO_2 zooids from VD contained 12.3% less $CaCO_3$. BMR zooids also possessed 10.3% less organic mass under high CO_2 compared with low CO_2 (P=0.042). $CaCO_3$ content varied significantly with population (P=0.003), CO_2 (P=0.040), autozooids (P<0.0001), population×autozooids (P<0.0001) and CO_2×autozooids (P<0.0001), with $CaCO_3$ content differing between high and low CO_2 levels within each population (BMR: P<0.0001; VD: P<0.0001). Under low CO_2, BMR colonies were significantly heavier than VD colonies in terms of both $CaCO_3$ (P=0.028) and organic mass (P=0.024). $CaCO_3$ masses were not significantly different between BMR and VD colonies held under high CO_2 (P=0.116)

Effects on skeletal magnesium and thickness

Bryozoan zooids from VD reared under high CO_2 exhibited 23.5% lower Mg/Ca_C ratios compared with those grown under low CO_2 conditions (P=0.0007; mean ratios=0.027 versus 0.035; s.e.m.=0.001, both treatments). Zooids grown under high CO_2 conditions also had thinner skeletal walls (P=0.059) than those from low CO_2 treatments, with the mean thickness of the primary frontal wall being reduced by 23.5% from 7.58 to 5.80 µm.

Organic covering response

The proportion of zooids exhibiting new organic coverings varied significantly with CO_2 treatment (P<0.0001), and both populations formed more organic coverings under high versus low CO_2 conditions (all pairwise comparisons, P<0.0001). For colonies in the high CO_2 treatment, organic coverings were 1.8 times more common in new zooids formed under high CO_2 compared with older zooids formed during the common garden period (P<0.0001). Colonies from VD raised under high CO_2 exhibited 5.3 times the number of organic coverings in zooids added during the treatment phase as compared with zooids that formed prior to high CO_2 exposure (P<0.0001). Colonies from VD had 2.1 times the number of zooids exhibiting organic covering formation in the high CO_2 treatment compared with colonies from BMR in the high CO_2 treatment (P=0.0006) and a 31% increase overall in the relative proportion of treatment phase zooids exhibiting this response under high CO_2 compared with BMR (P=0.003).

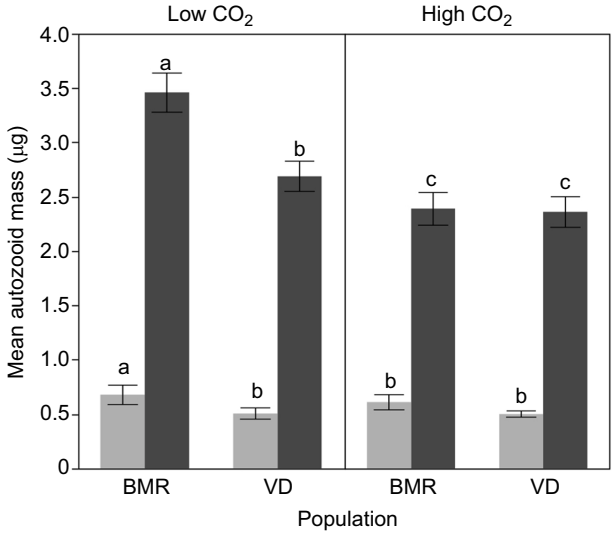

Fig. 5. Changes in the $CaCO_3$ and organic components of colony autozooids based on mass regressions under high and low CO_2. Light bars represent mean autozooid mass for organic components of zooids while dark bars represent mean $CaCO_3$ mass, each derived from linear regressions of whole colony mass against number of colony autozooids. Under high CO_2, zooids from both populations were composed of significantly less $CaCO_3$, while Bodega also showed a reduction in organic mass. Shared letters indicate group means that are not significantly different based on means comparisons of least squares group estimates (P>0.05). Error bars are ±1 s.e.m. Sample sizes: VD–high CO_2 n=32, VD–low CO_2 n=34, BMR–high CO_2 n=24, BMR–low CO_2 n=24.

Dissolution observations

Under high CO_2, we observed dissolution of the organic cuticle (Taylor et al., 2015) and possibly portions of the exterior calcified walls of zooids that were grown prior to exposure to the high CO_2 treatment (Fig. 1). Organic cuticle and the exterior walls of these zooids gradually receded through time, revealing the inner calcified layers of exterior walls. Sinuous remnants of the organic cuticle were observed on the surfaces of older zooids under SEM, indicating that the exterior organic framework of these zooids had broken down under high CO_2 conditions.

DISCUSSION

Our study demonstrates that native colonial bryozoans distributed along the northern California coast exhibit a surprisingly broad array of plastic responses to environmental change. In contrast to our initial prediction, we found that bryozoans grew faster under high CO_2 conditions. As discussed below, we observed that increases in overall growth were associated with shifts in the structure and composition of zooid skeletons and the proportion of reproductive zooids within colonies, reflecting the plastic nature of calcification and energy allocation in this colonial species (consistent with predictions 2 and 3; see Introduction).

Plasticity in reproductive investment

Life-history theory suggests that when resources are limited, organisms may balance investments in somatic maintenance (e.g. metabolism, physiological processes, immunity, repair functions) with investment in growth and reproduction (Roff, 1993; Stearns, 1992). Reproduction is energetically costly and is viewed as the most expensive life-history investment and trade-off in terms of the cost to future survival and fitness (Stearns, 1992). The effects of stress on reproduction have been widely documented in solitary organisms living in a variety of ecosystems (Schreck et al., 2001; Moore and Jessop, 2003; Petes et al., 2008; Fitzer et al., 2012), whereas the manner in which these life-history trade-offs manifest in colonial species is poorly understood.

In a short-term study, Pistevos et al. (2011) documented that reproductive investment in colonies of the European bryozoan *Celleporella hyalina* increased under increasing temperatures and decreasing pH. In the present study, we found the opposite pattern in *C. cornuta* from the northern California coast, with new colonial growth under high CO_2 being characterized by increased investment in feeding zooids relative to non-feeding reproductive zooids (both female and male). This outcome may represent a novel strategy in *Celleporella* populations adapted to episodic coastal upwelling, whereby colonies attempt to compensate for energetic stress related to periods of low pH by reallocating resources away from reproduction and into the growth of feeding autozooids to enhance caloric intake. Recent work indicates that increasing caloric intake may partially offset reductions in growth and calcification in other species under elevated CO_2 (Kroeker et al., 2016; Swezey et al., 2017). While this strategy might boost colony growth rates during episodic upwelling events, it may not convey a fitness benefit to bryozoans exposed to prolonged periods of low

Journal of Experimental Biology (2017) 220, 4399-4409 doi:10.1242/jeb.163436

saturation state conditions, as is expected to occur in the future ocean as low pH conditions become the norm (Gruber et al., 2012).

Adaptive alterations of zooid morphology

We also observed changes in the observed frequency of organic coverings, with a striking shift towards increased organic coverings in new generations of zooids formed by asexual budding under acidified conditions. We hypothesize that these organic coverings serve a protective function in *C. cornuta*, potentially reducing carbonate dissolution, as has been postulated for other bryozoan species (Lombardi et al., 2011). The heavy investment in organic coverings observed in younger generations of zooids could reflect either developmental canalization or adaptive energy partitioning. In the first case, it is possible that new zooids have morphological flexibility, whereas the formation of new organic coverings is rare or impossible in older zooids after they pass a critical stage of development and growth. Alternatively, the distribution of organic coverings under high CO_2 may reflect an energetic trade-off, with colonies exposed to stressful conditions actively diverting resources from older zooids (whose cuticles appear to deteriorate through time) to the formation of organic coverings in the younger portions of the colony. Such patterns of resource diversion to younger clonal generations are commonly observed in clonal plants (Alpert, 1991; Hutchings and Wijesinghe, 1997) and may be analogous to other patterns of resource translocation in invertebrates (Hughes, 2005).

Shifts in zooid calcification

While calcification pathways in bryozoans are diverse and mechanistically complex (Smith et al., 2006; Taylor et al., 2015), our mineralogical analyses revealed that *C. cornuta* colonies are constructed of low magnesium calcite (Mg/Ca_C=0.035). Given the temperature and alkalinity values maintained in our experiment, P_{CO_2} values of approximately 1700 µatm would be needed to induce kinetic dissolution of calcite in this species based on generalized solubility relationships for biogenic calcites with Mg/Ca_C=0.03 (Ries, 2011). Nevertheless, we saw significant decreases in colony carbonate mass under our treatment condition of 1254 µatm CO_2. If we assume that the carbonate masses of zooids laid down before the treatment phase were unaffected by high CO_2, as predicted by solubility curves for low Mg-calcite, new zooids in these colonies would need to be 46.5% and 43.9% lighter for BMR and VD, respectively, to account for observed reductions in total colony mass under high CO_2. The fact that zooids were thinner under high CO_2 suggests that this bryozoan can plastically reduce its investment in calcification under high CO_2, consistent with our third prediction. This trend might be related to the ability of *C. cornuta* to modulate the Mg content of zooid calcification under changing pH environments by apparently reducing the solubility of this material through the downregulation of skeletal Mg (Fig. 2). Recent work has documented similar plastic shifts in the mineralogical composition of gastropod shells under OA conditions, associated with a trade-off in inner shell density leading to the production of less dense but harder shells (Leung et al., 2017). In our study system, the full ecological implications of this downregulation of zooid mass and mineralogical change remain to be determined.

Adaptive divergence in colonial responses

Our long-term laboratory trials indicate that *C. cornuta* exhibits a variety of plastic responses to simulated future OA (Table 1), and that the nature of these plastic responses differs between the two populations examined. Although studies of additional replicate populations are needed, our findings are consistent with local adaptation to persistent oceanographic differences between these sites (Sanford and Kelly, 2011). Whereas both of our sites are within the upwelling zone of northern California, VD lies within a recognized center of upwelling, immediately south of Cape Mendocino (Magnell et al., 1990; Feely et al., 2008). Our field sensor data indicate that intertidal habitats at VD receive more consistent upwelling compared with BMR, resulting in more frequent exposure to low $\Omega_{aragonite}$ values at VD. VD is also characterized by significantly lower phytoplankton abundances than observed at BMR. This observation is consistent with trends observed at other centers of persistent upwelling activity, where upwelled waters just reaching the surface frequently move away from the coast before the development of large phytoplankton blooms (Pitcher et al., 2010). Thus, counter-gradient selection imposed by the low-food environment could favor VD bryozoans that can more efficiently convert normally limited energy into colony growth and maintenance through metabolic upregulation. New growth in VD colonies also showed a greater expression of organic coverings, which may protect against skeletal dissolution under acidified conditions, consistent with adaptation to greater CO_2 stress. Further, under low CO_2 conditions, VD colony autozooids were significantly lighter than colony autozooids from BMR (Fig. 5). VD colonies also showed a modest 12.3% reduction in carbonate mass under high CO_2 conditions while BMR colonies exhibited a 31% reduction. This suggests that colonies from VD may have adapted to recurring regional exposure to high CO_2 conditions by reducing overall investment in skeletal calcification, and they appear to be less affected by OA overall. In contrast, colonies from BMR, which may be adapted to higher food and lower CO_2 levels, grew more slowly and built zooids that were 23% heavier than those from VD under low CO_2 conditions. Colonies from BMR also showed an increased incidence of zooid degeneration under high CO_2 and a reduction in the average organic mass of zooids, changes that were not observed in VD colonies under these conditions, suggesting that under high CO_2, BMR colonies experience greater stress and physiological impairment.

Responses of colonial organisms to global environmental change

Coupled with prior studies, our results suggest that colonial organisms can employ a broad range of plastic responses that may afford special resilience to global environmental change. Analogous to our findings from bryozoans, physiological integration between the connected units of clonal plants has been shown to increase performance under challenging soil conditions and fluctuating

Table 1. Summary of directional population responses under high CO_2

Growth characteristic	Bodega (moderate upwelling)	Van Damme (high upwelling)
Zooids added	⇡	↑*
Female investment	↓	↓
Male investment	⇣	⇣
Zooid degeneration	↑	⇡
Organic coverings	↑	↑*
Carbonate mass	↓	↓
Organic mass	↓	⇣

Solid bold arrows indicate a significant (P<0.05) change under high CO_2 within a population, while dashed arrows represent non-significant directional changes. Asterisks indicate a significant difference between population responses under high CO_2.

levels of resource availability (Alpert, 1991; Price and Marshall, 1999; Roiloa and Retuerto, 2006). In these species, clonal units held in favorable microhabitats were able to provide nutrients and other resources to developing or stressed clones elsewhere in the colony. Studies of clonal plants have also documented shifts in the growth and identity of modular units in response to changing environmental conditions (Callaghan et al., 1992; Van Kleunen and Fischer, 2001), including resource diversions to vegetative tiller production and changes in allocations to sexual reproduction under simulated climate change (Stenström and Jónsdóttir, 1997; Jónsdóttir et al., 2005). Many colonial taxa, ranging from clonal plants to colonial marine invertebrates, show special flexibility in the timing of investment in reproduction, delaying or reducing investments in sexual reproduction when unfavorable conditions persist (Harvell and Grosberg, 1988). For example, some species of clonal plants possess a relatively fluid ability to shift resources towards or away from sexual reproduction with changes in prevailing temperatures, light levels and soil moisture content (Abrahamson, 1980; Stenström and Jónsdóttir, 1997). Our findings from bryozoans may therefore reflect general responses to environmental change that are representative of strategies observed in a much broader range of colonial taxa.

While assessments of standing level genetic variation and associated phenotypic diversity within species will continue to play a key role in predicting adaptive capacity under OA (Pespeni et al., 2013; Kim et al., 2013), our results also emphasize the importance of phenotypic plasticity in mediating responses to global environmental change, and particularly highlight the diverse strategies that may frequently be available to species with colonial growth forms. Although these plastic responses may partially buffer some colonial species against environmental changes, further studies are needed to fully understand the long-term demographic and ecological consequences of such shifts in morphology, colony function and reproductive investment. Our findings provide a cautionary note about the complexity of responses to global change, and add to recent calls (Chevin et al., 2010; Munday et al., 2013) for greater attention to the role that plasticity will play in mediating the responses of natural populations to global change.

APPENDIX

Field sensor deployments

We deployed custom-designed Durafet® pH sensors (Martz et al., 2010) adjacent to our bryozoan collection areas in the low-intertidal zone at Van Damme State Park (VD) and the Bodega Marine Reserve (BMR). Sensors were deployed from April to September of 2011–2013, recorded pH and temperature at 10-min intervals, and were typically returned to the laboratory every 4 to 8 weeks for maintenance and calibration. To identify potential anomalies, seawater bottle samples were taken for comparison with sensor records monthly at BMR and every other month at VD. Samples were preserved using $HgCl_2$, and pH, dissolved inorganic carbon (DIC) and total alkalinity (TA) of these samples were analyzed. Prior to re-deployment, each sensor unit was calibrated against both seawater and/or TRIS-based certified reference material provided by A. Dickson, Scripps Institute of Oceanography (La Jolla, CA, USA). Tidal height time series were used to identify when the sensors were exposed to air at low tide, and values from these periods were removed from the pH and temperature datasets. Occasional data spikes were removed using a ±4 standard deviation window filter. $\Omega_{aragonite}$ values from our results were calculated using the carbonate system software CO2SYS (Lewis and Wallace, 1998) by defining pH and temperature data as input variables, using an average salinity value of 33.5, and an average total alkalinity of 2200 µmol kg^{-1}. These salinity and alkalinity values were chosen based on local averages common at these sites as observed by the Ocean Margin Ecosystems Group for Acidification Studies (OMEGAS) consortium (Chan et al., 2017).

Analysis of chlorophyll concentrations from satellite data

We determined surface chl *a* concentrations at our two study sites using publicly available satellite imagery data collected by the Scripps Institution of Oceanography photobiology group (http://spg.ucsd.edu). We selected points forming a 1.75 km radius around our study locales, and merged data from SeaWiFS, MODIS, MERIS and VIIRS sensors, and calculated chl *a* concentrations with standard algorithms (Kahru et al., 2012). We generated average monthly sea surface chl *a* concentrations in 15-day increments during the months of April to October from 1998 to 2014. Pixel resolution of points analyzed was set at 1 km, and we included all cells where the center of the cell fell inside a 1.75 km radius.

Quantification of chlorophyll concentrations from bottle samples

To verify that the chl *a* concentrations at our two intertidal sites were accurately characterized by the satellite dataset, we also measured chl *a* concentrations in water samples from each location. On sampling dates, we collected water in acid-washed opaque HDPE sample bottles (250 ml) attached to a 2 m sampling pole. The bottle was rinsed in seawater three times, and then the sample was collected from ∼1 m below the surface of the water. A volume of 50 ml of seawater was immediately filtered from the bottles using 3 µm pore size combusted Whatman glass fiber filters (GF/F) at a low vacuum pressure (<5 mm Hg). Filters were placed in tubes and immediately frozen at −20°C for transport to the laboratory, where they were stored at −80°C until further processing. Samples were extracted for 12 h in 90% HPLC acetone held in darkness at −20°C. Chl *a* concentrations were then determined using a Turner Designs Model TD 70 fluorometer, following established methods (Aminot and Rey, 2000).

Spawning and culturing protocol

Celleporella cornuta colonies with gravid female reproductive zooids (ovicells) were collected on low-intertidal red algal blades (*Mazzaella* spp. and *Rhodymenia* sp.) from BMR and VD on 31 October 2012 and 11 November 2012, respectively. Colonies were transported to the Bodega Marine Laboratory for spawning, and each colony was placed at the bottom of an individual 120 ml plastic container (Starplex Scientific Leak Buster™) filled with 40 ml of 10 µm filtered UV-treated seawater (pre-equilibrated to 400 µatm CO_2, 15°C, pH=8.04). To prevent the settlement of coronate larvae on the algal substrate bearing the parent colony, algal blade material surrounding each colony was carefully trimmed away prior to the placement of colonies onto the bottoms of individual containers. To ensure that larvae settled onto transferable surfaces, the inner walls of each container were lined with acetate sheeting (Manríquez et al., 2001). Acetate sheets were conditioned under unfiltered running seawater for 2 weeks prior to use as settlement substrate. Containers with colonies were placed in a temperature-controlled incubator held at 15°C. Each container received aeration from an individual airline delivering ambient room air (390 µatm CO_2).

Following an initial 24-h exposure to darkness, colonies were exposed for 13 days to a 12 h:12 h light:dark cycle, using overhead fluorescent lighting in the temperature-controlled incubator to induce the episodic release of swimming coronate larvae. Larvae

Journal of Experimental Biology

Journal of Experimental Biology (2017) 220, 4399-4409 doi:10.1242/jeb.163436

settled on the experimental acetate substrate within 24 h of release from ovicells (D.S.S., personal observation). Parent colonies and experimental substrates with newly settled founding zooids (ancestrula) were transferred every other day into clean containers filled with pre-equilibrated filtered seawater held at 15°C. Unsettled larvae still swimming at the time of water changes were individually collected using a glass Pasteur pipette and transferred to the new containers along with individual parent colonies. Following each water change, concentrated suspensions of the live microalgae *Rhodomonas* sp. and *Isochrysis galbana* (approximately 30 cells μl^{-1}, with 15 cells μl^{-1} of each species) were fed to colonies in each container.

At the end of the 13-day light:dark spawning period, sections of acetate sheeting bearing individual newly settled colonies (approximately two to five zooids in size) were removed and affixed to 5×5 cm polycarbonate squares using a pinpoint drop of cyanoacrylate (Manríquez et al., 2001). Each polycarbonate square had been previously attached to a polycarbonate tube suspended from the lid of a new 120 ml sample container. Each colony was oriented vertically in the center of each container to reduce the buildup of colony feces. Individual colonies in experimental containers were then transferred to our flow-through CO_2 system, and the colonies were reproductively isolated for the remainder of the experiment.

Live algal cultures of the phytoplankton species *Rhodomonas* sp. and *I. galbana* were continuously maintained at the Bodega Marine Laboratory during the course of the experiment in order to feed colonies. During feedings, aliquots of these cultures were centrifuged at low speed and algal cells were re-suspended in 0.35 µm filtered seawater to create concentrated solutions. A hemocytometer was used to quantify algal cell concentrations, and this solution was added proportionately to experimental containers. Water delivery pumps were shut off for 1 h during each feeding to allow colonies time to filter feed at these high cell concentrations before resuming water flow in the system. All experimental containers were replaced with clean containers weekly to reduce the accumulation of dead algal cells. Every 2 weeks, each colony was removed and cleaned gently with a soft artist's brush to prevent surface fouling. Between each cleaning, brushes were immersed in distilled water for a minimum of 5 min and then rinsed with filtered seawater to reduce the possibility of live sperm transfer between colonies.

Flow-through CO_2 culturing system

Temperature control of experimental containers in our flow-through system was maintained by partially immersing the bottom half of the experimental containers in controlled water baths. Each bath had aquarium pumps to recirculate water past titanium 500 W heaters (Jehmco TSHW-500-20). The water baths were held at approximately 15°C using individual temperature controllers (OMEGA Engineering CN76020) linked to heaters. Overhead PVC manifolds delivered water to each container via individual 3.2 mm plastic tubing lines, and each tube terminated in an irrigation dipper (0.95 liters h^{-1}, Drip Works Miniquart Drippers). Drippers were held flush with the bottom of experimental containers to create directional water flow from the bottom to the top of each container, facilitating suspension of algal cells for bryozoan filter feeding. Containers were sealed with threaded plastic lids, each of which possessed an embedded dripping tube, allowing for visual verification of water flow through the experimental containers. Dripper function and water flow in each experimental container was assessed daily, and any drippers showing reduced flow rates were immediately replaced.

Treatment seawater was delivered to two overhead manifolds using two aquarium pumps (Lifegard Quiet One 3000), each drawing from a sump receiving a continuous supply of filtered UV-treated seawater and treatment gas. Sump 1 (680 liter capacity) received a constant delivery of 25 standard liters per minute (SLPM) treatment air mix at 350 µatm CO_2. Carbon dioxide concentrations were quantified using an infrared CO_2 gas analyzer (S151, Qubit Systems). Sump 2 (340 liters) received a constant supply of 1150 µatm CO_2 treatment air delivered at 35 SLPM. Air was mixed with treatment seawater using sets of fine bubble diffusers (Membrane Check Valve Fine Bubble Diffuser, Cole Parmer). The temperature of each sump was held at 15°C, regulated using 1000-W titanium aquarium heaters attached to OMEGA controllers, and water was circulated using submersible pumps. Incoming unequilibrated 10 µm filtered UV-treated seawater was delivered continuously to each sump at approximately 1.5 SLPM.

Treatment air delivered to each sump was generated by blending dry CO_2-free air with pure CO_2 gas using pairs of digital mass flow controllers (MFC) for both air (SmartTrak 50C, 0–50 l min^{-1}, Sierra Instruments) and CO_2 [SmartTrak 50C, 0–100 sccm (standard cubic centimeters per minute), Sierra Instruments]. CO_2-free air was supplied to the air MFCs by delivering atmospheric air to an air dryer/CO_2 scrubber (CAS2, Puregas LLC) using two linked, oil-free air compressors (Thomas 1207PK80). Pure CO_2 was supplied to MFCs using a high-pressure industrial cylinder of pure CO_2 (Airgas LLC Pure Clean CO_2). Flows of both gases were set digitally via a laptop computer and mixed in individual lines, such that custom atmospheric values could be created by digitally turning flows of either gas up or down relative to one another to create and then deliver the desired treatment gas level to the fine bubble diffusers in the sumps.

Quantifying mass

Prior to weighing, live bryozoan colonies were removed from the experimental apparatus, immersed in distilled water and brushed clean. Surface water was then gently removed using Kimwipes and colonies were carefully scraped from their acetate growing surfaces into individual pre-weighed foil weigh boats (pre-ashed at 500°C for 3 h). Colonies were left to dry for 24 h at 30°C and then weighed on a microbalance (Sartorius Ultramicro) to determine their total mass, which included organic and carbonate components of colony zooids. Colonies in weigh boats were then placed in crucibles in a muffle furnace (Thermo Scientific FB1415M) and heated to 460°C for 4 h to volatilize organic components of colony zooids. Colonies were then re-weighed to determine their total carbonate skeletal mass.

The organic component mass of each colony was calculated by subtracting final colony carbonate mass from initial total colony mass. We then performed linear regressions of zooid counts against carbonate and organic mass. Outliers were identified and excluded using jackknife distances for each population×CO_2 group at the 0.05 level (using either organic or carbonate mass with ovicells and autozooids as multivariate factors). Ovicells were a non-significant predictor of colony mass in individual population×CO_2 regressions, while number of autozooids was highly significant (all $P<0.0001$), so end autozooid number was used as the independent variable in colony mass regressions.

Acknowledgements

We thank M. Carroll, K. Laughlin, G. Baxter, N. Botto, F. Chan, K. Griffith, D. Hall, L. Heidenreich, J. Hosfelt, T. Landers, J. Lankford, J. Newman, S. Roeske, L. Rose, A. Russell, P. Stull and T. Woods for their help with field and laboratory work and analyses during the course of this project. We also thank N. Willits and M. Whalen for statistical advice, and the University of California Natural Reserve System and State

Parks of California for access to these study sites. T. Bell provided useful assistance with satellite chlorophyll analyses, and J. Stachowicz, R. Grosberg, E. Rivest and two anonymous reviewers provided helpful comments on the manuscript.

Competing interests
The authors declare no competing or financial interests.

Author contributions
Conceptualization: D.S.S., E.S.; Methodology: D.S.S., J.R.B., A.T.N., T.M.H., B.G., E.S.; Software: D.S.S., A.T.N.; Validation: D.S.S., J.R.B., A.T.N., T.M.H., B.G., E.S.; Formal analysis: D.S.S., J.R.B., A.T.N., E.S.; Investigation: D.S.S., J.R.B., A.T.N., E.S.; Resources: D.S.S., J.R.B., T.M.H., B.G., E.S.; Data curation: D.S.S., J.R.B., A. T.N.; Writing - original draft: D.S.S., E.S.; Writing - review & editing: D.S.S., J.R.B., A. T.N., T.M.H., B.G., E.S.; Visualization: D.S.S., J.R.B., A.T.N., B.G., E.S.; Supervision: D.S.S., T.M.H., B.G., E.S.; Project administration: D.S.S., T.M.H., B.G., E.S.; Funding acquisition: D.S.S., T.M.H., B.G., E.S.

Funding
This research was supported by the National Science Foundation [grants OCE-0927255, OCE-1041089, OCE-1220648 and DGE-0841297], the University of California Multicampus Research Programs and Initiatives (MRPI), and an NSF Graduate Research Fellowship to D.S.S.

Data availability
Data are available from the Dryad Digital Repository (Swezey et al., 2017): https://doi.org/10.5061/dryad.3gt37

Supplementary information
Supplementary information available online at http://jeb.biologists.org/lookup/doi/10.1242/jeb.163436.supplemental

References
Abrahamson, W. G. (1980). Demography and vegetative reproduction. In *Demography and Evolution in Plant Populations* (ed. O. T. Solbrig), pp. 89-106. Oxford, UK: Blackwell.
Alpert, P. (1991). Nitrogen sharing among ramets increases clonal growth in *Fragaria chiloensis*. *Ecology* **72**, 69-80.
Aminot, A. and Rey, F. (2000). Standard procedure for the determination of chlorophyll *a* by spectroscopic methods. ICES techniques in marine environmental sciences. ICES, Copenhagen. Available at: www.ices.dk/ocean/procedures/timeschl.pdf.
Barton, A., Hales, B., Waldbusser, G. G., Langdon, C. and Feely, R. A. (2012). The Pacific oyster, *Crassostrea gigas*, shows negative correlation to naturally elevated carbon dioxide levels: implications for near-term ocean acidification effects. *Limnol. Oceanogr.* **57**, 698-710.
Caldeira, K. and Wickett, M. E. (2005). Ocean model predictions of chemistry changes from carbon dioxide emissions to the atmosphere and ocean. *J. Geophys. Res.* **110**, C09S04.
Callaghan, T. V., Carlsson, B. Å., Jónsdóttir, I. S., Svensson, B. M. and Jonasson, S. (1992). Clonal plants and environmental change: introduction to the proceedings and summary. *Oikos* **63**, 341-347.
Chan, F., Barth, J. A., Blanchette, C. A., Byrne, R. H., Chavez, F., Cheriton, O., Feely, R. A., Friederich, G., Gaylord, B., Gouhier, T. et al. (2017). Persistent spatial structuring of coastal ocean acidification in the California Current System. *Sci. Rep.* **7**, 2526.
Chevin, L.-M., Lande, R. Mace, G. M. (2010). Adaptation, plasticity, and extinction in a changing environment: towards a predictive theory. *PLoS Biol.* **8**, e1000357.
Easley, R. A. and Byrne, R. H. (2012). Spectrophotometric calibration of pH electrodes in seawater using purified m-cresol purple. *Environ. Sci. Technol.* **46**, 5018.
Feely, R. A., Sabine, C. L., Hernandez-Ayon, J. M., Ianson, D. and Hales, B. (2008). Evidence for upwelling of corrosive “acidified” water onto the continental shelf. *Science* **320**, 1490-1492.
Fitzer, S. C., Caldwell, G. S., Close, A. J., Clare, A. S., Upstill-Goddard, R. C. and Bentley, M. G. (2012). Ocean acidification induces multi-generational decline in copepod naupliar production with possible conflict for reproductive resource allocation. *J. Exp. Mar. Biol. Ecol.* **418**, 30-36.
Gaylord, B., Kroeker, K. J., Sunday, J. M., Anderson, K. M., Barry, J. P., Brown, N. E., Connell, S. D., Dupont, S., Fabricius, K. E., Hall-Spencer, J. M., et al. (2015). Ocean acidification through the lens of ecological theory. *Ecology* **96**, 3-15.
Gordon, D. P. (1977). The aging process in bryozoans. In *Biology of Bryozoans* (ed. R.M. Woollacott and R. L. Zimmer), pp. 335-375. New York: Academic Press.
Gruber, N., Hauri, C., Lachkar, Z., Loher, D., Frölicher, T. L. and Plattner, G.-K. (2012). Rapid progression of ocean acidification in the California Current System. *Science* **337**, 220-223.
Harvell, C. D. and Grosberg, R. K. (1988). The timing of sexual maturity in clonal animals. *Ecology* **69**, 1855-1864.
Hoffmann, A. A. and Sgrò, C. M. (2011). Climate change and evolutionary adaptation. *Nature* **470**, 479-485.
Hofmann, G. E., Evans, T. G., Kelly, M. W., Padilla-Gamiño, J. L., Blanchette, C. A., Washburn, L., Chan, F., McManus, M. A., Menge, B. A., Gaylord, B. (2014). Exploring local adaptation and the ocean acidification seascape – studies in the California Current Large Marine Ecosystem. *Biogeosciences* **11**, 1053-1064.
Hughes, R. N. (2005). Lessons in modularity: the evolutionary ecology of colonial invertebrates. *Sci. Mar.* **69**, 169-179.
Hughes, D. J. and Hughes, R. N. (1986). Life history variation in *Celleporella hyalina* (Bryozoa). *Proc. R. Soc. B Biol. Sci.* **228**, 127-132.
Hutchings, M. J. and Bradbury, I. K. (1986). Ecological perspectives on clonal perennial herbs. *Bioscience* **36**, 178-182.
Hutchings, M. J. and Wijesinghe, D. K. (1997). Patchy habitats, division of labour and growth dividends in clonal plants. *Trends Ecol. Evol.* **12**, 390-394.
Jacobs, D. K., Haney, T. A. and Louie, K. D. (2004). Genes, diversity, and geologic process on the Pacific coast. *Annu. Rev. Earth Planet. Sci.* **32**, 601-652.
Jónsdóttir, I. S., Khitun, O. and Stenström, A. (2005). Biomass and nutrient responses of a clonal tundra sedge to climate warming. *Botany* **83**, 1608-1621.
Jump, A. S. and Penuelas, J. (2005). Running to stand still: adaptation and the response of plants to rapid climate change. *Ecol. Lett.* **8**, 1010-1020.
Kahru, M., Kudela, R. M., Manzano-Sarabia, M. and Mitchell, B. G. (2012). Trends in the surface chlorophyll of the California Current: merging data from multiple ocean color satellites. *Deep Sea Res. Part II.* **77**, 89-98.
Kim, T. W., Barry, J. P. and Micheli, F. (2013). The effects of intermittent exposure to low-pH and low-oxygen conditions on survival and growth of juvenile red abalone. *Biogeosciences* **10**, 7255-7262.
Kroeker, K. J., Kordas, R. L., Crim, R., Hendriks, I. E., Ramajo, L., Singh, G. S., Duarte, C. M. and Gattuso, J.-P. (2013). Impacts of ocean acidification on marine organisms: quantifying sensitivities and interaction with warming. *Glob. Change Biol.* **19**, 1884-1896.
Kroeker, K. J., Sanford, E., Rose, J. M., Blanchette, C. A., Chan, F., Chavez, F. P., Gaylord, B., Helmuth, B., Hill, T. M., Hofmann, G. E., et al. (2016). Interacting environmental mosaics drive geographic variation in mussel performance and predation vulnerability. *Ecol. Lett.* **19**, 771-779.
Leung, J. Y. S., Russell, B. D. and Connell, S. D. (2017). Mineralogical plasticity acts as a compensatory mechanism to the impacts of ocean acidification. *Environ. Sci. Technol.* **51**, 2652-2659.
Lewis, E. and Wallace, D.W.R. (1998). *Program Developed for CO2 System Calculations*. ORNL/CDIAC-105. Carbon Dioxide Information Analysis Center, Oak Ridge National Laboratory, U.S. Department of Energy, Oak Ridge, Tennessee.
Lombardi, C., Rodolfo-Metalpa, R., Cocito, S., Gambi, M. C. and Taylor, P. D. (2011). Structural and geochemical alterations in the Mg calcite bryozoan *Myriapora truncata* under elevated seawater pCO2 simulating ocean acidification. *Mar. Ecol.* **32**, 211-221.
Magnell, B., Bray, N., Winant, C., Greengrove, C., Largier, J., Borchardt, J., Bernstein, R. and Dorman, C. (1990). Convergent shelf flow at Cape Mendocino. *Oceanography* **3**, 4-11.
Manríquez, P., Hughes, R. and Bishop, J. (2001). Age-dependent loss of fertility in water-borne sperm of the bryozoan *Celleporella hyalina*. *Mar. Ecol. Prog. Ser.* **224**, 87-92.
Martz, T. R., Connery, J. G. and Johnson, K. S. (2010). Testing the Honeywell Durafet® for seawater pH applications. *Limnol. Oceanogr. Methods* **8**, 172-184.
McKinney, F. K. and Jackson, J. B. C. (1989). *Bryozoan Evolution*. Chicago, IL: University of Chicago Press.
Moore, I. T. and Jessop, T. S. (2003). Stress, reproduction, and adrenocortical modulation in amphibians and reptiles. *Horm. Behav.* **43**, 39-47.
Morris, P. A. (1976). Middle Pliocene temperature implications based on the Bryozoa *Hippothoa* (Cheilostomata, Ascophora). *J. Paleontol.* **50**, 1143-1149.
Morris, P. A. (1980). *The Bryozoan Family Hippothoidae (Cheilostomata-Ascophora), with Emphasis on the Genus Hippothoa*. Monograph of the Allan Hancock Foundation, Vol. 10, pp. 1-115. Los Angeles, CA: University of Southern California.
Morse, J. W., Andersson, A. J. and Mackenzie, F. T. (2006). Initial responses of carbonate-rich shelf sediments to rising atmospheric pCO_2 and ‘ocean acidification’: role of high Mg-calcites. *Geochim. Cosmochim. Acta* **70**, 5814-5830.
Munday, P. L., Warner, R. R., Monro, K., Pandolfi, J. M. and Marshall, D. J. (2013). Predicting evolutionary responses to climate change in the sea. *Ecol. Lett.* **16**, 1488-1500.
Orr, J. C., Fabry, V. J., Aumont, O., Bopp, L., Doney, S. C., Feely, R. A., Gnanadesikan, A., Gruber, N., Ishida, A., Joos, F. et al. (2005). Anthropogenic ocean acidification over the twenty-first century and its impact on calcifying organisms. *Nature* **437**, 681-686.
Pespeni, M. H., Sanford, E., Gaylord, B., Hill, T. M., Hosfelt, J. D., Jaris, H. K., LaVigne, M., Lenz, E. A., Russell, A. D., Young, M. K. et al. (2013). Evolutionary change during experimental ocean acidification. *Proc. Natl Acad. Sci. USA* **110**, 6937-6942.

Petes, L. E., Menge, B. A. and Harris, A. L. (2008). Intertidal mussels exhibit energetic trade-offs between reproduction and stress resistance. *Ecol. Monogr.* **78**, 387-402.
Pinheiro, J. and Bates, D. (2000). *Mixed-Effects Models in S and S-PLUS*. New York: Springer.
Pistevos, J. C. A., Calosi, P., Widdicombe, S. and Bishop, J. D. D. (2011). Will variation among genetic individuals influence species responses to global climate change? *Oikos* **120**, 675-689.
Pitcher, G. C., Figueiras, F. G., Hickey, B. M. and Moita, M. T. (2010). The physical oceanography of upwelling systems and the development of harmful algal blooms. *Prog. Oceanogr.* **85**, 5-32.
Pörtner, H. O. (2008). Ecosystem effects of ocean acidification in times of ocean warming: a physiologist's view. *Mar. Ecol. Prog. Ser.* **373**, 203-217.
Price, E. A. C. and Marshall, C. (1999). Clonal plants and environmental heterogeneity: an introduction to the proceedings. *Plant Ecol.* **141**, 3-7.
Ries, J. B. (2011). Skeletal mineralogy in a high-CO_2 world. *J. Exp. Mar. Biol. Ecol.* **403**, 54-64.
Roff, D. (1993). *Evolution of Life Histories: Theory and Analysis*. New York: Springer Science & Business Media.
Roiloa, S. R. and Retuerto, R. (2006). Physiological integration ameliorates effects of serpentine soils in the clonal herb Fragaria vesca. *Physiol. Plant* **128**, 662-676.
Sabine, C. L., Feely, R. A., Gruber, N., Key, R. M., Lee, K., Bullister, J. L., Wanninkhof, R., Wong, C., Wallace, D. W., Tilbrook, B. et al. (2004). The oceanic sink for anthropogenic CO2. *Science* **305**, 367-371.
Sánchez, J. A., Aguilar, C., Dorado, D. and Manrique, N. (2007). Phenotypic plasticity and morphological integration in a marine modular invertebrate. *BMC Evol. Biol.* **7**, 122.
Sanford, E. and Kelly, M. W. (2011). Local adaptation in marine invertebrates. *Ann. Rev. Mar. Sci.* **3**, 509-535.
Schreck, C. B., Contreras-Sanchez, W. and Fitzpatrick, M. S. (2001). Effects of stress on fish reproduction, gamete quality, and progeny. *Aquaculture* **197**, 3-24.
Smith, A. M., Key, M. M. and Gordon, D. P. (2006). Skeletal mineralogy of bryozoans: taxonomic and temporal patterns. *Earth-Sci. Rev.* **78**, 287-306.
Stearns, S. C. (1992). *The Evolution of Life Histories*. Oxford: Oxford University Press.
Stenström, A. and Jónsdóttir, I. S. (1997). Responses of the clonal sedge, *Carex bigelowii*, to two seasons of simulated climate change. *Glob. Change Biol.* **3**, 89-96.
Stuefer, J. F. (1996). Potential and limitations of current concepts regarding the response of clonal plants to environmental heterogeneity. *Plant Ecol.* **127**, 55-70.
Swezey, D. S., Bean, J. R., Ninokawa, A. T., Hill, T. M., Gaylord, B. and Sanford, E. (2017). Interactive effects of temperature, food and skeletal mineralogy mediate biological responses to ocean acidification in a widely distributed bryozoan. *Proc. R. Soc. B* **284**, 20162349.
Swezey, D. S., Bean, J. R., Hill, T. M., Gaylord, B. P., Ninokawa, A. T. and Sanford, E. D. (2017). Data from: Plastic responses of bryozoans to ocean acidification. *Dryad Digital Repository*. https://doi.org/10.5061/dryad.3gt37.
Taylor, P. D., Lombardi, C. and Cocito, S. (2015). Biomineralization in bryozoans: present, past and future. *Biol. Rev.* **90**, 1118-1150.
Van Kleunen, M. and Fischer, M. (2001). Adaptive evolution of plastic foraging responses in a clonal plant. *Ecology* **82**, 3309-3319.
Waddington, C. H. (1942). Canalization of development and the inheritance of acquired characters. *Nature* **150**, 563-565.

Sea Water Property	Low CO_2	High CO_2	Significance
Temperature (°C)	15.308 (15.305, 15.312)	15.319 (15.316, 15.323)	P<0.0001
Salinity	33.72 (33.619, 33.821)	33.71 (33.635, 33.791)	P=0.3669
TA (µmol kg_{sw}^{-1})	2249 (2245, 2253)	2250 (2246, 2254)	P=0.7388
DIC_{calc} (µmol kg_{sw}^{-1})	2221 (2216, 2226)	2315 (2309, 2322)	P<0.0001
pH_T	8.04 (8.03, 8.06)	7.60 (7.58, 7.63)	P<0.0001
pCO_{2CALC}	400 (389, 412)	1254 (1213, 1296)	P<0.0001
$\Omega_{aragonite}$	2.34 (2.29, 2.40)	.98 (.90, 1.07)	P<0.0001
$\Omega_{calcite}$	3.65 (3.57, 3.74)	1.53 (1.40, 1.66)	P<0.0001

Table S1. Experimental chemistry conditions.

Mean carbonate system parameter values, 95% confidence intervals and significance of difference between low and high CO_2 treatments during the course of the study. Partial pressure of CO_2 (pCO_{2calc}), aragonite and calcite saturation state ($\Omega_{aragonite/calcite}$) and total dissolved inorganic carbon (DIC_{calc}) were calculated from the measured values of total alkalinity (TA), pH total (pHT), temperature and salinity. The significance of differences between CO_2 treatments were assessed using Student's t-test.

Response Variable	Response Group	LS Means Estimate	SE	Lower 95% CI	Upper 95% CI		Group Comparison	Difference	SE	DF	t-Ratio	p	Lower 95% CI	Upper 95% CI
Total Zooids Added														
	BMR Low CO_2	101.48	13.89	72.34	130.63		BMR Low - VD High CO_2	-53.85	18.46	46.90	-2.92	**0.005***	-90.99	-16.72
	BMR High CO_2	108.46	14.42	78.19	138.74		BMR High - VD High CO_2	-46.88	18.86	46.90	-2.49	**0.016***	-84.82	-8.94
	VD Low CO_2	131.11	12.32	103.83	158.39		VD Low - VD High CO_2	-24.23	11.90	46.90	-2.04	**0.047***	-48.17	-0.29
	VD High CO_2	155.34	12.16	128.41	182.28		BMR Low - VD Low CO_2	-29.62	18.56	46.90	-1.60	0.117	-66.97	7.73
							BMR High - VD Low CO_2	-22.65	18.96	46.90	-1.19	0.238	-60.79	15.50
							BMR Low-BMR High CO_2	-6.98	13.49	46.90	-0.52	0.607	-34.11	20.16
Female Investment: $\log_{10}(O+1)/([A_F+A_M+A_B]+1)$:														
	BMR Low CO_2	-0.66	0.05	-0.77	-0.55		BMR Low-BMR High CO_2	0.12	0.05	21.00	2.30	**0.031***	0.01	0.23
	BMR High CO_2	-0.78	0.05	-0.89	-0.67		VD Low-VD High CO_2	0.11	0.04	13.90	2.35	**0.034***	0.01	0.21
	VD Low CO_2	-0.67	0.04	-0.77	-0.58		BMR Low-VD High CO_2	0.12	0.07	25.10	1.78	0.087	-0.01	0.27
	VD High CO_2	-0.79	0.04	-0.88	-0.69		BMR High-VD Low CO_2	-0.10	0.07	25.50	-1.52	0.141	-0.25	0.03
							BMR Low-VD Low CO_2	0.01	0.07	25.10	0.20	0.845	-0.13	0.15

							BMR High-VD High CO_2	0.004	0.07	25.50	0.06	0.954	-0.14	0.14
Male Investment: $A_M/(A_M+A_F)$:														
	BMR Low CO_2	0.41	0.03	0.35	0.47		BMR Low - VD High CO_2	0.08	0.04	18.77	2.08	0.051	0.01	0.16
	Co	0.36	0.03	0.30	0.42		BMR Low - BMR High CO_2	0.05	0.03	18.77	1.80	0.087	-0.01	0.12
	VD Low CO_2	0.36	0.03	0.31	0.42		VD Low - VD High CO_2	0.03	0.03	18.77	1.23	0.235	-0.02	0.09
	VD High CO_2	0.33	0.03	0.28	0.38		BMR Low- VD Low CO_2	0.05	0.04	18.77	1.20	0.245	-0.03	0.13
							BMR High - VD High CO_2	0.03	0.04	18.77	0.68	0.506	-0.05	0.11
							BMR High - VD Low CO_2	-0.01	0.04	18.77	-0.21	0.837	-0.09	0.07
Degenerated Zooid %														
	BMR Low CO_2	0.19	0.02	0.15	0.24		BMR Low - BMR High CO_2	-0.05	0.02	17.50	-2.17	**0.044***	-0.09	0.01
	BMR High CO_2	0.24	0.02	0.19	0.29		BMR Low - VD High CO_2	-0.05	0.03	17.50	-1.78	0.091	-0.12	0.01
	VD Low CO_2	0.23	0.02	0.19	0.27		BMR Low - VD Low CO_2	-0.04	0.03	17.50	-1.19	0.249	-0.10	0.03
	VD High CO_2	0.25	0.02	0.20	0.29		VD Low - VD High CO_2	-0.02	0.02	17.50	-1.00	0.332	-0.06	0.02
							BMR High - VD Low CO_2	0.01	0.03	17.50	0.31	0.757	-0.06	0.07
							BMR High - VD High CO_2	-0.01	0.03	17.50	-0.28	0.780	-0.07	0.06
Colony $CaCO_3$ Weight (10^{-5} g)														
	BMR Low CO_2	64.49	2.11	60.18	68.81		VD Low- VD High CO_2	11.01	2.00	29.17	5.49	**<0.001***	6.91	15.11
	BMR High CO_2	51.69	2.18	47.23	56.15		BMR Low - BMR High CO_2	12.80	2.03	29.17	6.31	**<0.001***	8.66	16.95
	VD Low CO_2	57.96	1.99	53.81	62.10		BMR Low - VD High CO_2	17.54	2.88	29.17	6.09	**<0.001***	11.66	23.43
	VD High CO_2	46.95	2.08	42.68	51.22		BMR Low - VD Low CO_2	6.54	2.83	29.17	2.31	**0.028***	0.75	12.32
							BMR High	-6.27	2.8	29.	-	**0.03**	-	-0.38

							- VD Low CO_2		8	17	2.18	**7***	12.16	
							BMR High - VD High CO_2	4.74	2.93	29.17	1.62	0.116	-1.25	10.73
Colony Organic Weight (10^{-5} g)														
	BMR Low CO_2	16.86	2.35	12.19	21.53		BMR Low - VD High CO_2	7.64	3.02	88.0	2.53	**0.013***	1.60	13.65
	BMR High CO_2	10.06	2.312	5.47	14.66		BMR Low - BMR High CO_2	6.80	3.30	88.0	2.06	**0.042***	0.24	13.35
	VD Low CO_2	9.96	1.86	6.26	13.66		BMR Low – VD Low CO_2	6.90	3.00	88.0	2.30	**0.024***	0.94	12.86
	VD High CO_2	9.22	1.9	5.45	12.99		BMR High - VD High CO_2	0.84	2.99	88.0	0.28	0.778	-5.10	6.79
							VD Low - VD High CO_2	0.74	2.66	88.0	0.28	0.782	-4.50	6.03
							BMR High - VD Low CO_2	0.11	2.97	88.0	0.04	0.972	-5.80	6.01
% of Zooids with Organic Coverings														
	BMR Low CO_2	0.01	0.01	-0.01	0.02		BMR Low - VD High CO_2	-0.09	0.01	19.16	-10.97	**<0.001***	-0.10	-0.07
	BMR High CO_2	0.09	0.01	0.08	0.10		BMR Low - BMR High CO_2	-0.08	0.01	19.16	-9.69	**<0.001***	-0.10	-0.07
	VD Low CO_2	0.01	0	0	0.02		VD Low - VD High CO_2	-0.08	0.01	19.16	-11.90	**<0.001***	-0.10	-0.07
	VD High CO_2	0.09	0.01	0.08	0.10		BMR High - VD Low CO_2	0.08	0.01	19.16	9.91	**<0.001***	0.06	0.10
							BMR Low - VD Low CO_2	0	0.01	19.16	-0.60	0.553	-0.02	0.01
							BMR High - VD High CO_2	0	0.01	19.16	-0.43	0.674	-0.02	0.01
% of Zooids with Organic Coverings in Treatment Phase Growth														
	BMR Low CO_2	0.0006	0.01	-0.01	0.02		BMR Low - VD High	-0.13	0.01	25.51	-13.0	**<0.001***	-0.15	-0.10

							CO_2				6			
	BMR High CO_2	0.09	0.01	0.07	0.1		VD Low - VD High CO_2	-0.13	0.01	25.51	-14.69	**<0.001***	-0.15	-0.10
	VD Low CO_2	0	0.01	-0.01	0.01		BMR Low - BMR High CO_2	-0.09	0.01	25.51	-8.41	**<0.001***	-0.12	-0.06
	VD High CO_2	0.13	0.01	0.12	0.14		BMR High - VD Low CO_2	0.09	0.01	25.51	9.12	**<0.001***	0.06	0.12
							BMR High - VD High CO_2	-0.04	0.01	25.51	-3.93	**0.003***	-0.07	-0.01
							BMR Low - VD Low CO_2	0	0.01	25.51	0.07	0.999	-0.03	0.03
Mg/Ca_c														
	VD Low CO_2	0.035	0.001	0.032	0.038		VD Low - VD High CO_2	0.008	0.002	12.0	4.53	**0.0007***	0.004	0.01
	VD High CO_2	0.027	0.001	0.024	0.029									
Skeletal Wall Thickness (µm)														
	VD Low CO_2	7.53	0.58	6.29	8.78		VD Low - VD High CO_2	1.68	0.82	13.81	2.05	0.059	-0.08	3.43
	VD High CO_2	5.85	0.58	4.61	7.09									

Table S2. Least squares group means estimates and significance assessments derived from mixed effects model output for colony response variables.